6212

Inhibition of ATM-dependent checkpoint control and DNA double-strand break repair enhances the efficacy of ATR inhibitors

Audrey Turchick[1†], Astrid Zimmermann[2], Li-Ya Chiu[1], Heike Dahmen[2], **Brian Elenbaas[1*]**, Frank T. Zenke[1], Andree Blaukat[2†], Lyubomir T. Vassilev[1†]

[1]Research Unit Oncology, EMD Serono, Billerica, MA, USA; [2]Research Unit Oncology, the healthcare business of Merck KGaA, Darmstadt, Germany

*Presenting author (brian.elenbaas@emdserono.com); †affiliation at the time of study

CONCLUSIONS

- **Ataxia telangiectasia and Rad3-related kinase inhibition (ATRi) blocks the ATR signaling pathway, but simultaneously activates the ataxia telangiectasia mutated (ATM) pathway**
- **ATRi causes an ATM/p53-dependent G1 cell cycle arrest which diminishes the cytotoxicity and DNA lesions caused by ATRi**
- **Combination of ATRi and ATMi caused synergistic cell killing in cancer cell lines *in vitro* and increased efficacy in tumor models *in vivo***
- **These results suggest a novel and efficacious DNA damage response (DDR) inhibitor combination approach for cancer therapy[1]**

INTRODUCTION

- ATR is activated by replication stress, stalled replication forks and single-stranded DNA[2]. Activated ATR phosphorylates CHK1 which stabilizes replication forks, induces cell cycle arrest checkpoints and promotes homologous recombination (HR) repair. ATRi blocks these functions, but also activates ATM as a compensatory pathway
- ATM is activated by double-stranded DNA breaks (DSBs) and phosphorylates multiple substrates including CHK2 and p53 to cause cell cycle arrest and promote HR repair[3]. ATMi causes cell death in combination with DSB-inducing therapies such as radiotherapy and certain chemotherapies[3]

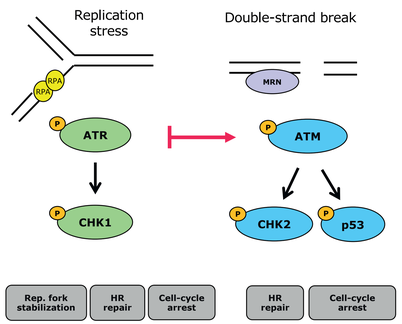

ATR, ataxia telangiectasia and Rad3-related; **ATM**, ataxia telangiectasia mutated; **HR**, homologous recombination; **MRN**, MRE11–RAD50–NBS complex; **RPA**, replication protein-A.

DDR inhibitors used in this study		
ATRi	Berzosertib/M6620/ VE-822	Gartisertib/M4344
ATMi	M3541	M4076

RESULTS

Figure 1. ATRi berzosertib inhibits p-CHK1, but simultaneously activates the ATM pathway

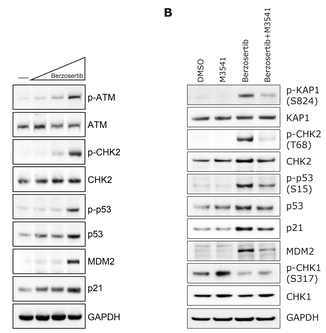

A549 non-small cell lung cancer (NSCLC) cells were treated with **A**) ATRi berzosertib at increasing concentrations (50, 100, 200 nM) or **B**) ATMi M3541 (1 μM), ATRi berzosertib (200 nM) or the combination, for 24 hrs. Lysates were analyzed by Western blot for ATM and ATR signaling pathway components.

RESULTS

Figure 2. ATRi causes a p53-mediated G1 cell cycle arrest that is abrogated by addition of ATMi

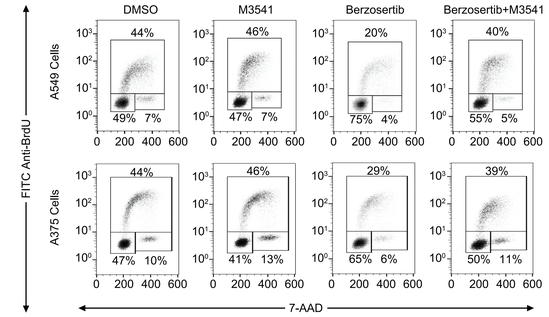

A549 or A375 cells were treated with ATMi M3541, ATRi berzosertib, or the combination for 24 hrs. Cell cycle analysis was done by BrdU/7-AAD flow cytometry.

Figure 3. ATRi + ATMi causes enhanced cancer cell death and synergy that is dependent on the ATM-p53 pathway

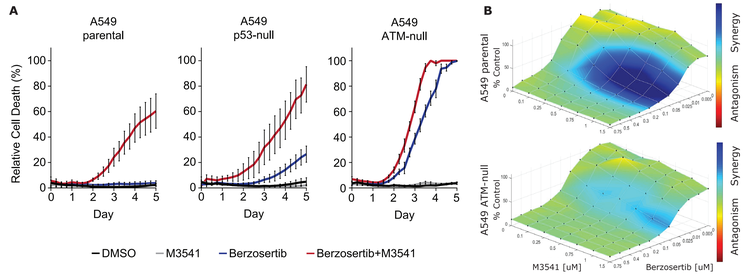

A. A549 isogenic cell lines (parental, p53-null, ATM-null) were treated with M3541 (1 μM), berzosertib (200 nM), or the combination, starting at Day 0, and analyzed by IncuCyte live cell imaging. Relative cell death was calculated from the number of cells positively stained with CytoTox dye normalized to confluence. Error bars represent the standard error of mean (SEM).

B. Bliss synergy plots were generated from CellTiter-Glo viability results. A549 parental and ATM-null cells were treated for 5 days with titrations of M3541 and berzosertib. Bliss synergy was determined by Combenefit software.

Figure 4. ATMi enhanced chromosomal damage of ATRi as cells progress through the cell cycle with unrepaired DSBs

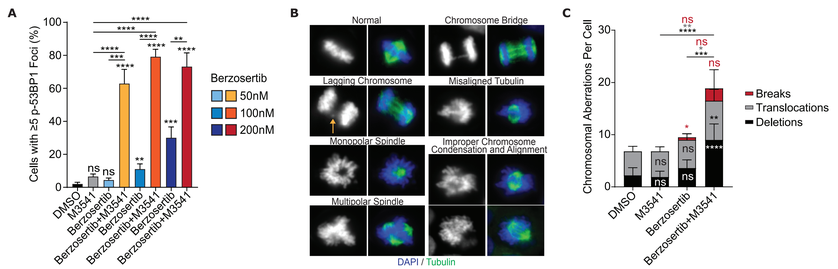

A. A549 cells were treated with ATRi, ATMi or the combination for 24 hrs, followed by immunofluorescence (IF) of p-53BP1 foci, a marker of DSBs.

B. IF images of abnormal mitotic events in unsynchronized A549 cells 24 hrs after M3541 (1 μM) + berzosertib (200 nM) treatment.

C. Chromosomal spectral karyotyping analysis was conducted on 10 metaphase spreads from cells treated with M3541 (1 μM), berzosertib (200 nM) or the combination for 24 hrs. The graph shows the total number of chromosomal aberrations per metaphase spread and the occurrence of breaks, translocations or deletions.

For **A**, **C**, Error bars represent the SEM and ****p<0.0001, ***p<0.001, **p<0.01, and *p<0.05 by unpaired t-test.

Figure 5. ATMi M4076 synergizes with ATRis gartisertib or berzosertib in cancer cells *in vitro*

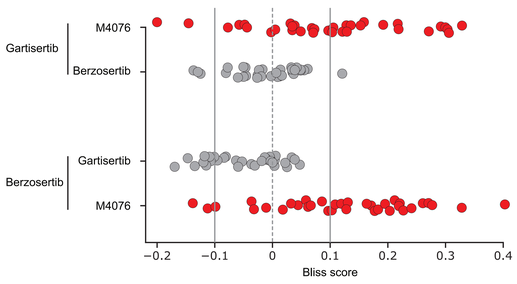

Combination benefit of ATRis (gartisertib, berzosertib) and ATMi (M4076) in a panel of 34 randomly selected cancer cell lines. Cell lines were incubated with drugs for 5 days and their viability was determined by sulforhodamin-B. Bliss excess was calculated per drug and cell line and plotted (strong synergy >0.1; weak-to-moderate additivity/antagonism >-0.1 to 0.1; strong antagonism <-0.1).

Figure 6. ATMi enhances the efficacy of ATRi in cell line-derived (CDX) models *in vivo*

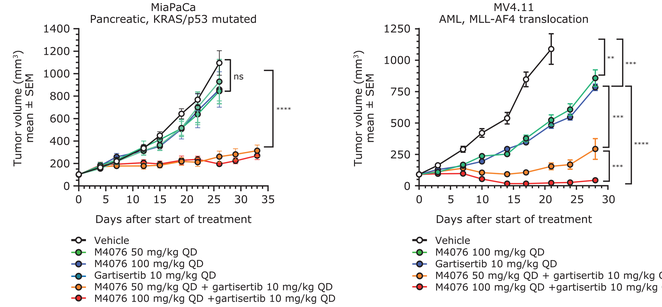

Mice bearing MiaPaca or Mv4-11 xenografts were treated with ATRi gartisertib (10 mg/kg), ATMi M4076 (50 or 100 mg/kg), or the combination. Drugs were given daily (QD), orally, throughout the study period. Gartisertib was given 1 h after M4076. Tumor volumes are shown as mean ± SEM (n=10 mice/group). The combination was well tolerated in both studies based on body weight changes. ****p<0.0001, ***p<0.001, **p<0.01 by unpaired t-test for the indicated comparisons. **AML**, acute myeloid leukemia; **SEM**, standard error of mean.

Figure 7. ATMi enhances the efficacy of ATRi in a panel of 26 patient-derived xenograft (PDX) models of TNBC *in vivo*

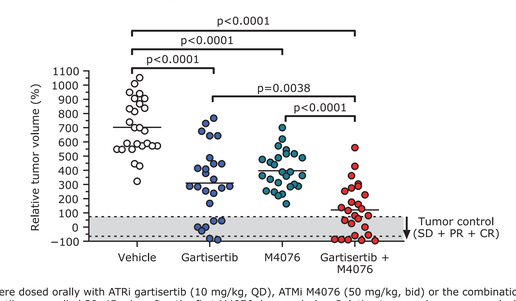

Mice were dosed orally with ATRi gartisertib (10 mg/kg, QD), ATMi M4076 (50 mg/kg, bid) or the combination. Gartisertib was applied 30–45 mins after the first M4076 dose each day. Relative tumor volumes were calculated from the median of each treatment group (n=3 mice/group) when the controls reached 800 mm³. Applying tumor volume adapted RECIST criteria, gartisertib showed a tumor control rate [including stable disease (SD), partial response (PR), complete response (CR)] of ~27% (7/26) and an objective response rate (PR, CR) of ~8% (2/26). The combination treatment had a tumor control rate of 42% (11/26) and an objective response rate of 19% (5/26).

References: 1. Turchick A, Zimmermann A, et al. 2023 (submitted); **2.** Blackford N, Jackson P. *Mol Cell* 2017;66:801–17; **3.** Zimmermann A, Zenke FT, et al. *Mol Cancer Ther* 2022; 21(6):859-870.

Disclosures: AT and **LTV** were employees of EMD Serono, Billerica, MA, USA, at the time of study. **LYC**, **BE** and **FTZ** are employees of EMD Serono, Billerica, MA, USA. **AZ** and **HD** are employees of the healthcare business of Merck KGaA, Darmstadt, Germany. **AB** was an employee of the healthcare business of Merck KGaA, Darmstadt, Germany at the time of study.

Acknowledgements: This research was sponsored by the healthcare business of Merck KGaA, Darmstadt, Germany (CrossRef Funder ID: 10.13039/100009945). Editorial assistance was provided by Mario Pahl of Bioscript Group, Macclesfield, UK, and funded by the healthcare business of Merck KGaA, Darmstadt, Germany.

Presented at the American Association for Cancer Research Annual Meeting 2023 | April 14–19 | Orlando, FL, USA